IGNITION BEHAVIOUR OF RECIRCULATING SPRAY FLAMES USING MULTIPLE SPARKS

T. Marchione, S.F. Ahmed and E. Mastorakos
tm346@cam.ac.uk
Hopkinson Laboratory, Engineering Department, University of Cambridge, UK

Abstract

This paper quantifies the increase in ignitability offered by the use of multiple sparks in an n-heptane spray in a swirling recirculating flow typical of a liquid-fuel burner. The spark was located close to the combustion chamber enclosure, i.e. far from the spray injection, and was relatively large and long compared to the length and time scales of the flow so as to simulate the placement and characteristics of a gas turbine combustor surface igniter. Spark discharges each lasting 8ms at 100Hz were created in the 5mm gap between two stainless steel 1mm diameter electrodes connected to a coil. The spark sequence lasted from approximately 1 to 5s, hence a total of about 100 to 500 sparks were used. It was found that a long spark sequence increases the ignition probability, which reached a maximum of 100% at an axial distance of about one burner inlet diameter. Ignition in the outer recirculation zone was possible only with spark sequences of duration longer than 2s, while all sequences tested did not produce ignition with the spark downstream of about two burner diameters. Imaging with a fast camera showed that small flame kernels emanate very often from the spark, which can be stretched as far as 20mm from the electrodes by the turbulent motion. Successful overall ignition occurs at a random time from the spark initiation and is associated with kernels that propagate towards the bluff body to stabilize the flame. The results are related to the air and droplet velocity patterns measured by Phase and Laser Doppler Anemometry and demonstrate that the energy deposited by multiple sparks can have a spatially far-reaching effect to initiate combustion.

IGNITION BEHAVIOUR OF RECIRCULATING SPRAY FLAMES USING MULTIPLE SPARKS

T. Marchione, S.F. Ahmed and E. Mastorakos
tm346@cam.ac.uk
Hopkinson Laboratory, Engineering Department, University of Cambridge, UK

Abstract

This paper quantifies the increase in ignitability offered by the use of multiple sparks in an n-heptane spray in a swirling recirculating flow typical of a liquid-fuel burner. The spark was located close to the combustion chamber enclosure, i.e. far from the spray injection, and was relatively large and long compared to the length and time scales of the flow so as to simulate the placement and characteristics of a gas turbine combustor surface igniter. Spark discharges each lasting 8ms at 100Hz were created in the 5mm gap between two stainless steel 1mm diameter electrodes connected to a coil. The spark sequence lasted from approximately 1 to 5s, hence a total of about 100 to 500 sparks were used. It was found that a long spark sequence increases the ignition probability, which reached a maximum of 100% at an axial distance of about one burner inlet diameter. Ignition in the outer recirculation zone was possible only with spark sequences of duration longer than 2s, while all sequences tested did not produce ignition with the spark downstream of about two burner diameters. Imaging with a fast camera showed that small flame kernels emanate very often from the spark, which can be stretched as far as 20mm from the electrodes by the turbulent motion. Successful overall ignition occurs at a random time from the spark initiation and is associated with kernels that propagate towards the bluff body to stabilize the flame. The results are related to the air and droplet velocity patterns measured by Phase and Laser Doppler Anemometry and demonstrate that the energy deposited by multiple sparks can have a spatially far-reaching effect to initiate combustion.

Introduction

The initiation of a flame through a spark discharge in a flammable mixture is one of the fundamental problems in combustion that have been studied very thoroughly by analysis [1] and experiment [2]. A large amount of effort has also been devoted to the effects of flow, and of the turbulence in particular, in the successful ignition. This work has shown, in general terms, that to ignite a flammable mixture one needs to deliver enough energy to raise a region of characteristic size proportional to the laminar flame thickness to the adiabatic flame temperature [1] and that the presence of turbulence can be detrimental to ignition due to straining of the flame kernel that may hence be extinguished [2,3].

In the context of igniting a realistic spray flame, such as that in a liquid-fuelled combustor, these insights must be extended in three directions. First, a proper account of the presence of liquid droplets must be included. The review by Aggarwal [4] discusses trends from various sources and in particular from the work of Ballal and Lefebvre that showed that the minimum ignition energy of a droplet-laden air flow, with the droplets relatively uniformly dispersed, increases over the value expected from ignition of a gaseous-air mixture of the same total equivalence ratio due to the energy necessary to evaporate the droplets [2,5-

8]. Second, in a realistic combustor the droplets are not uniformly dispersed and hence the presence of equivalence ratio local non-uniformities must be taken into account. Hence, in the context of ignition of non-premixed combustion with gaseous fuels, recent work on laminar diffusion flame simulations [9], Direct Numerical Simulations of turbulent mixing layers [10], and experiments [11-12] has been performed that demonstrates that spark-ignition of turbulent non-premixed combustion has a stochastic nature, with the randomness arising through the mixture fraction, as first suggested in Ref. [13], but additionally through the strain rate fluctuations at the spark location [11]. Finally, successful ignition of a realistic combustor involves not only the successful generation of a flame kernel following the energy deposition by the spark, but also flame propagation and overall stability of the flame. This aspect of gaseous and spray ignition has been little studied so far and has been denoted as the "Phase 2" of a gas turbine combustor ignition process [2]. Our previous work [14,15] visualized ignition processes in swirling and non-swirling gaseous and spray flames by a single spark and the ignition probability spatial distribution showed quite unexpected shapes, which could nevertheless be explained through analysis of local mixture fraction and velocity measurements. In particular, it was demonstrated that regions with high ignition probability are those where the mixture is not far from the stoichiometric, the flow velocity is favourable for upstream flame propagation, and the local turbulence weak enough or the mixture strong enough so that the small flame kernels initiated from the spark are not extinguished. Hence, the spark location and parameters such as energy, gap and duration affect not only the kernel creation, but also the subsequent propagation [11] due to the coupling with the probability of having a favourable local velocity or not. For example, a wide gap or a long spark duration increase the chances of favourable conditions for kernel propagation that then results in a higher ignition probability of the whole flame [11-12].

Practical ignition of a gas turbine combustor attracts attention from engine manufacturers because the current trend towards lean operation makes flame initiation more difficult. In aviation engines, ignition is accomplished by surface-discharge igniters that deposit large amounts of energy over long periods of time (of the order of seconds) and create large sparks [16] that penetrate into the flow. However, still, flame propagation and establishment is not always achieved. In an effort to understand this problem better, in this paper we examine ignition processes from large, repeated sparks in a laboratory-scale swirling spray flame whose ignition from a small single spark has already been studied [15]. The fundamental differences between the present work and that in Ref. [15] are that here the spark is 5mm instead of 2mm, the electrode gap is located close to the enclosure wall rather than in the bulk of the flow in order to mimic the placement of gas turbine igniters that are surface-mounted, and that we use multiple rather than single sparks in order to reproduce the long sparking sequences used in practice. It should be mentioned that the ignition with a single spark was not possible at all at the location of the present spark, i.e. close to the wall [15]. The use of multiple sparks is one of the keys to providing successful ignition when the spark is located away from the bulk of the flow, as we will see here, and this may be considered the main focal point of this work.

Experimental methods

The experimental apparatus is depicted in Fig. 1, which shows the burner assembly, the fuel line and the exhaust system. The burner consists of a 350mm long circular duct of D=35mm inner diameter, fitted with a conical bluff body of diameter 25mm giving a blockage ratio of 50% (Fig. 1). The fuel injection system consists of a pressure swirl atomiser and a feeding tank pressurised by nitrogen at 0.5MPa gauge pressure. The nozzle exit

diameter is 0.15mm; the spray cone angle is 60°, while the fuel flow rate is 0.025kg/min. N-heptane is used as fuel. The combustion chamber consists of a 70mm inner diameter glass tube 80mm in length. The air enters from the annular open area between the outer duct wall and the bluff body. Swirl is imparted by static swirl vanes at 60° with respect to the flow axis along the flow passage between the inner and outer ducts (the geometrical swirl number is about 1.4). The direction of the air swirl is clockwise when looking at the nozzle from the combustion chamber. The global equivalence ratio was Φ=0.64 with a bulk air velocity U=17m/s.

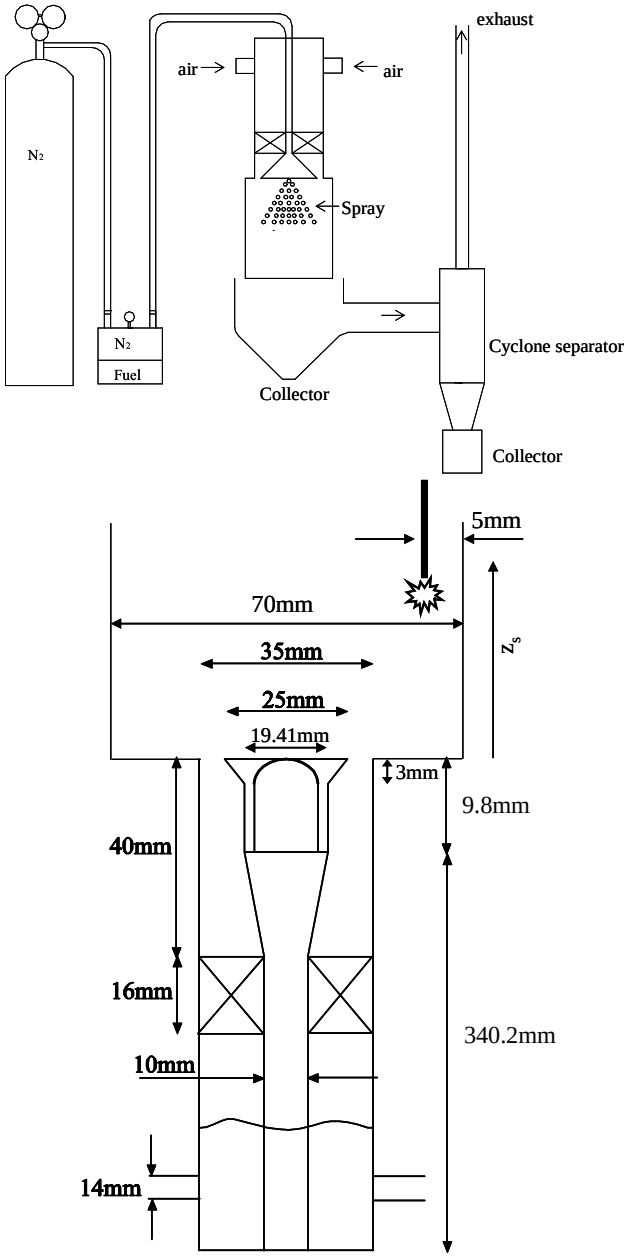

Fig. 1 Overall experimental arrangement for spark-ignition experiments (top) and schematic of the burner (bottom). Dimensions in mm. Z_s is the axial location of the spark.

The ignition unit used in this study was taken from a commercial spark system. It consists of a Fida T35/E AC-DC transfomer, which produces sparks with 14kV and 20mA peak voltage and current respectively. This unit continuously delivers sparks lasting for 8ms separated by a 2ms break, i.e. it gives multiple sparks at 100Hz. The spark sequence used here lasted approximately 1 to 5s, hence a total of about 100 to 500 sparks were delivered. The

electrical energy delivered by the circuit was about 3J for a 1s sequence duration, which corresponds to an energy per spark discharge of 30mJ, which is higher than the minimum ignition energies of both gaseous heptane-air mixtures [17] and droplet-air mixtures of iso-octane [2] and n-heptane [4; quoting various sources] at approximately the same *U* and Sauter mean diameter as in this burner.

The sparks were created in the 5mm gap between two stainless steel 1mm diameter electrodes. The electrodes were located 5mm from the combustion chamber wall with their axes normal to the spray direction and hence the spark was aligned in the azimuthal direction at a radius 30mm (Fig. 1). The two electrodes were set-up on a test stand that allowed the spark itself to translate in a vertical line parallel to the burner axis to within 0.1mm resolution. For each axial position of the spark (Z_s is the spark's distance from the burner inlet), 50 independent spark sequences of fixed duration were performed and the percentage of events resulting in a flame establishment gave the ignition probability.

Fast images of the spark sequence and the subsequent ignition event were acquired with a Phantom V4.2 digital high-speed CMOS camera. The spark only (i.e. without flow of air or fuel) was imaged at 59,000 frames per second in order to determine its duration and frequency mentioned previously. The movies of ignition were captured with 4,000fps and exposure time 250μs, which is short enough to capture the rate of growth of the ignition kernel. The camera could visualize the whole combustion chamber and was placed so as to have a front view of the spark. Phase Doppler Anemometry (PDA) was used for the simultaneous measurement of droplet size and axial velocity in inert condition (i.e. before sparking), while the LDV option of the PDA system in backscattering mode was used for the air velocity, which was measured without the presence of the spray with seeding provided by a smoke generator. The optical probe was mounted on a three-dimensional traversing system with stepper motors in order to allow for a computer-controlled traversing of the flow. These measurements will assist the interpretation of the ignition images and the ignition probability results.

Results and Discussion

Flow patterns

The axial and the tangential components of the mean air velocity are reported in Fig. 2. The former is available only from one side of the burner and hence half the contour is given. The highest velocities are found at the radial coordinates between 12 and 18mm corresponding at the annular exit from the burner face. The central area is characterised from low and negative velocity, in contrast to the side area that has positive values. The large recirculation zone created by the bluff body and the swirl is evident and this causes a rapid decrease in axial velocity and a wide angle of the flow coming out of the burner inlet. The mean swirl component of the velocity, plotted on the right side of the Fig. 2, shows a marked symmetry of the air flow field: negative values on the right and positive on the left.

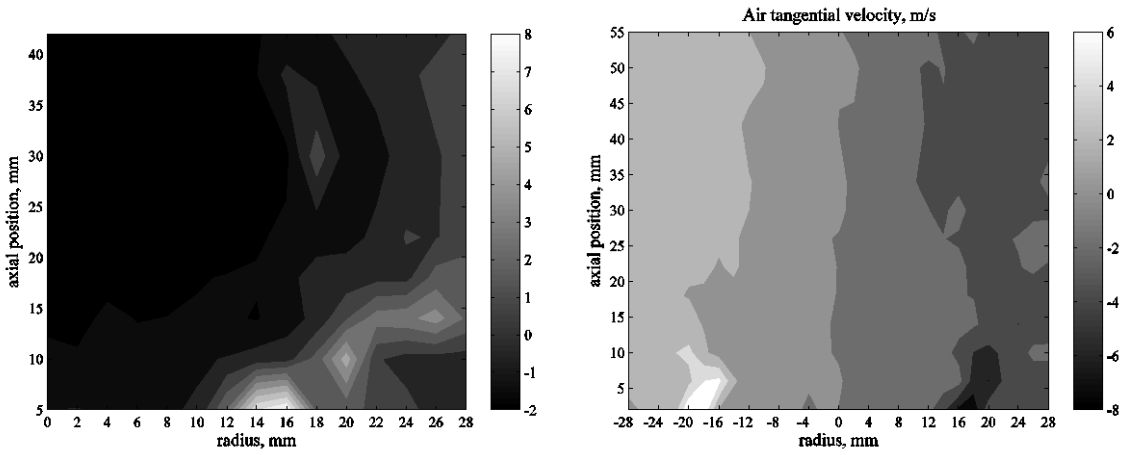

Fig. 2 Contour of the mean axial and tangential air velocity in m/s.

Extrapolating the results shown in Fig. 2 to the spark radial location (r=30mm) implies that for all axial placements of the spark the mean swirl velocity is about 4m/s and the mean axial velocity is negative up to about z=10mm and reaches its highest positive value at about z=15mm. The r.m.s. fluctuating velocities (not shown here) are about 1.0 to 1.5m/s, which imply very high local relative turbulent intensities at the spark position. Using a typical turbulent eddy lengthscale of 5mm (the distance of the spark from the wall), we have a large-scale turbulent timescale of about 5ms and a typical convection time of this eddy past the spark gap of about 1ms, both of which are smaller than the spark discharge duration of 8ms. Hence we expect large velocity and mixture fluctuations in the flow passing by the electrode gap during the time of energy deposition by the spark.

Figure 3 depicts the mean axial velocity contour of the droplets. This plot shows the central recirculation zone, where the direction of the velocity is toward the exit of the burner, and the annular jet area where the velocity values are positive and high. The data do not extend to the spark radial position, but with extrapolation we can infer that the mean droplet velocity at all spark locations along the chamber enclosure is, in general, positive.

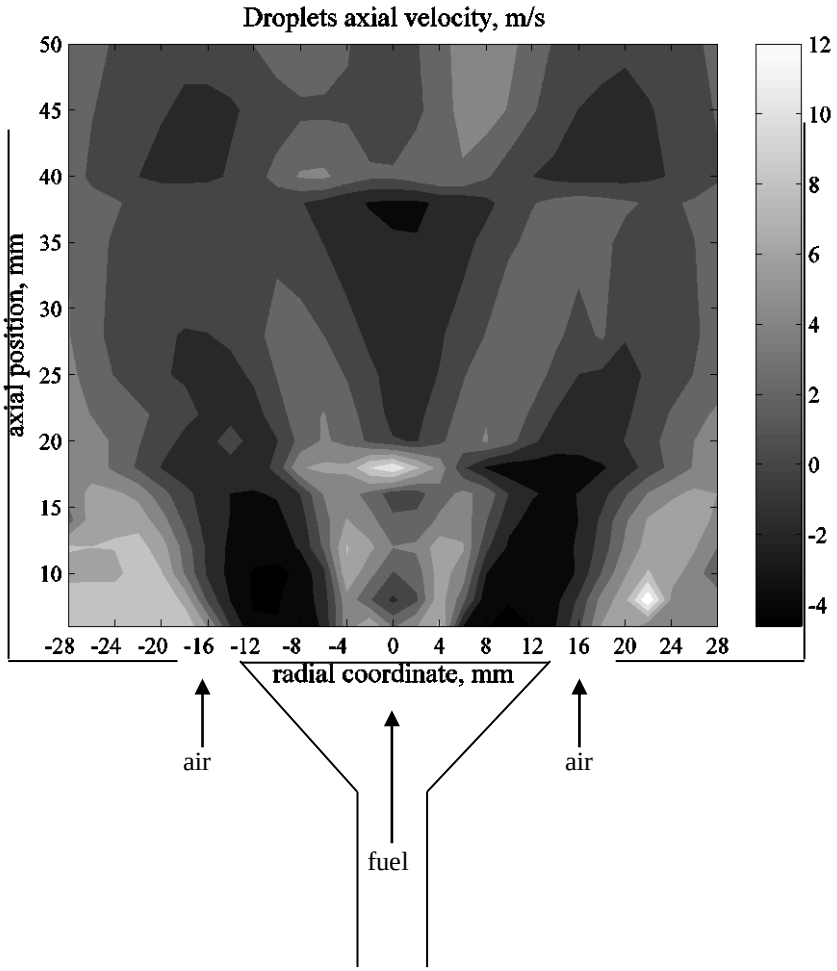

Fig. 3 Contour of the mean axial velocity of the droplets in m/s.

The Sauter mean diameter is plotted in Fig. 4. High values (around 65-75 μm) are found in the central region close to the exit of the nozzle up to 12mm from the burner; then they start to decrease (around 20-30μm) until the axial position 22mm. From this location until 50mm the values increase again (around 60 μm). N-heptane, unlike diesel fuel or kerosene, evaporates substantially at atmospheric conditions and hence the increase of the Sauter mean diameter with distance can be related to the quick evaporation of the small droplets that are more likely to get trapped in the recirculation zone. The contours at the largest radius for which data are available show that the Sauter mean diameter increases with distance along the wall (extrapolating the data from *r*=28mm to the spark radial position of 30mm).

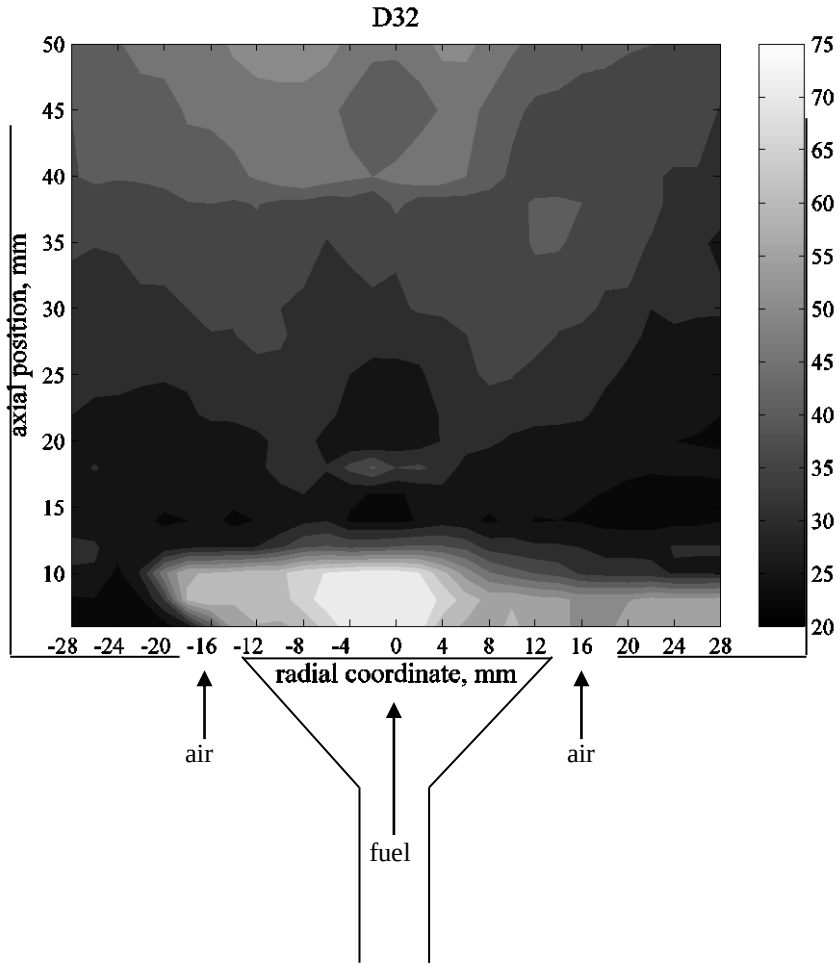

Fig. 4 Contour of the Sauter mean diameter in μm.

Visualization of ignition and flame propagation

Figure 5 shows selected images from the fast-camera films of the ignition phenomena for different axial positions of the spark along the enclosure.

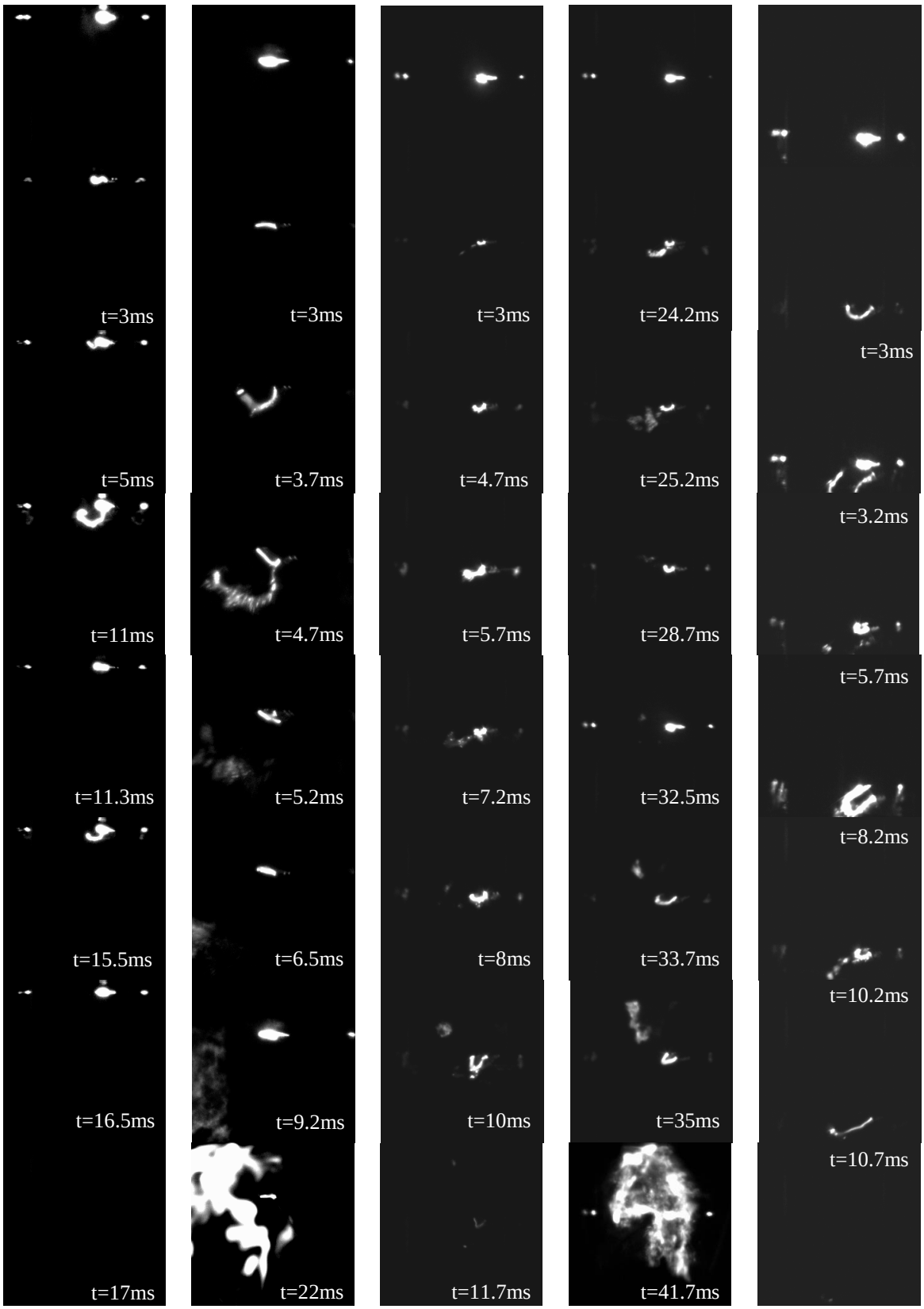

Z_s=5mm **(a)** Z_s=15mm **(b)** Z_s=35mm **(c)** Z_s=35mm **(d)** Z_s=65mm **(e)**

Fig. 5 Fast-camera images of successful and failed ignition events with a 2s spark sequence. The air and spray come from the top, while the swirling motion at the spark position is to the left. Front view of the spark which is placed at the indicated position.

For these images the spark sequence was continuous for 2 seconds. For all images, the flow comes from the top, the electrode gap and hence the spark is horizontal and the camera sees the spark through the flow. Time t=0 refers to the beginning of the film, which is later than the beginning of the sparking sequence, since the image acquisition and the sparking sequence were not synchronized.

In column (a) of Fig. 5, the spark is placed at Z_s=5mm. We see strong light emission from the spark itself that remains attached to the electrodes for as long as we are sparking and occasionally a flame kernel grows (11ms), but then it starts to decrease until it completely disappears. This behaviour is typical of failed spark sequences at this axial position. In Fig. 5(b), the spark is now at Z_s=15mm. At 3ms, the spark is visible, while at 3.7ms we probably see a distorted discharge due to the turbulent flow. At 4.7ms, a large kernel is visible that seems to have grown from the spark of the previous image, while a new spark has been established between the electrodes. The spark distortion and the initial movement of the kernel are mainly in the flow direction (downwards and towards the left). At 5.2ms and later the kernel has grown and eventually propagates back towards the burner until the stabilization of the flame. Note that during this time (e.g. from 4.7 to 22ms) the spark has kept operating, but no new flame kernel has appeared to come from it.

In Fig. 5c, after a short time of the sequence of the spark, a kernel comes off the spark line (e.g. the image at 7.2ms) and moves toward the burner. Since we observe a front view of the spark, the leftwards and upwards motion of the kernel suggests that the flame kernel is carried by the swirl and eventually propagates upstream. However, since we cannot tell the kernel's radial position, we cannot decide on the magnitude of the air axial velocity at the kernel's position and hence it is not clear if the kernel is advected upstream or propagates against the flow. The kernel grows to a few mm in size (image at 10ms), but it eventually disappears. After a little while, with the spark at 24.2ms (Fig. 5d), a new kernel grows off the spark and seems to get advected by the swirling flow in the downstream and tangential direction. At 25.2ms, the kernel is visible. At 28.7ms, the old kernel seems to have left the imaged region, but a new small and faint kernel seems to have been created next to the spark. This kernel moves slowly, is slightly more visible at 32.5ms, grows steadily (33.7 and 35ms) and eventually the whole flame is established. Again, the spark gets distorted by the flow and keeps delivering energy, but combustion kernels are not created continuously from it. The characteristic of films with successful ignition from this location is the capture of the flame kernel by the swirl and the upstream movement of a small kernel that manages to grow while in the central region of the image. Finally, in Fig. 5e we see highly distorted sparks (e.g. at 1.2, 3.0, and 8.2ms) and small kernels that are convected downstream (e.g. images at 3.0 and 10.2ms) and eventually leave the imaged domain. The snapshot at 10.7ms shows no kernel and the absence of spark: it happened that this image coincided with the 2ms delay between the end of a spark with the beginning of the next one. This spark is at Z_s=65mm. This position is too far from the burner, so there is little chance for the flame to be assisted by the turbulent fluctuations to even momentarily move towards the burner, which seems to be the key phenomenon for successful overall flame ignition (Fig. 5d, images between 32.5 and 35ms).

The successful flame kernel starts off the spark at random times relative to the spark initiation. Using as a characteristic residence time in the burner the ratio D/U, we estimate it to be 2ms. This time is too short compared to the duration of each of the sparks and orders of magnitude shorter than the whole spark sequence. However, the time taken for individual kernels to grow and ignite most of the flame is of the same order as the residence time.

We have not observed kernels off the spark moving against the swirling motion, which implies a flame propagation speed smaller than the swirl velocity (about 4m/s on average). Hence, it is unlikely that the flame can propagate against the incoming flow at the annular jet

that is faster than this (Fig. 2). It is rather more likely that the kernel is advected to the root of the flame by the mean recirculating flow and the turbulence while inside the recirculation zone. The presence of swirl increases the chances that the flame can spread inside the recirculation zone and later ignite the whole flame.

All the fast-camera images show that the flow greatly affects the shape of the spark and momentary distortions of even 10-20mm from the electrodes have been observed, possibly due to the large magnitude of the turbulent velocity fluctuations. The images at 4.7ms in Fig. 5b and 8.2ms in Fig. 5e are examples of such large spark distortions. These large fluctuations and the possibility of kernels that propagated upstream of the spark (e.g. Fig. 5c, 10ms) despite eventually failing, suggest that continuous spark discharge will increase the probability of ignition by increasing the chances of establishing a hot environment around the spark. In a sense, the fluctuating motion of the spark and the failed kernels can help prepare the incoming mixture to achieve combustion, e.g. by pre-vapourizing it and hence reducing the minimum ignition energy. Hence, we expect that a longer spark sequence can increase the probability of ignition. This is consistent with gas turbine practice [2] and this trend is quantified in more detail below.

Ignition probability

The probabilistic nature of ignition of non-premixed systems was mentioned before [4] and was studied in detail in Refs. [11-15]. Here, we show additional data for this when the spark is large. Figure 6 depicts the ignition probability for different axial positions Z_s and at different spark sequences between 1 and 5s.

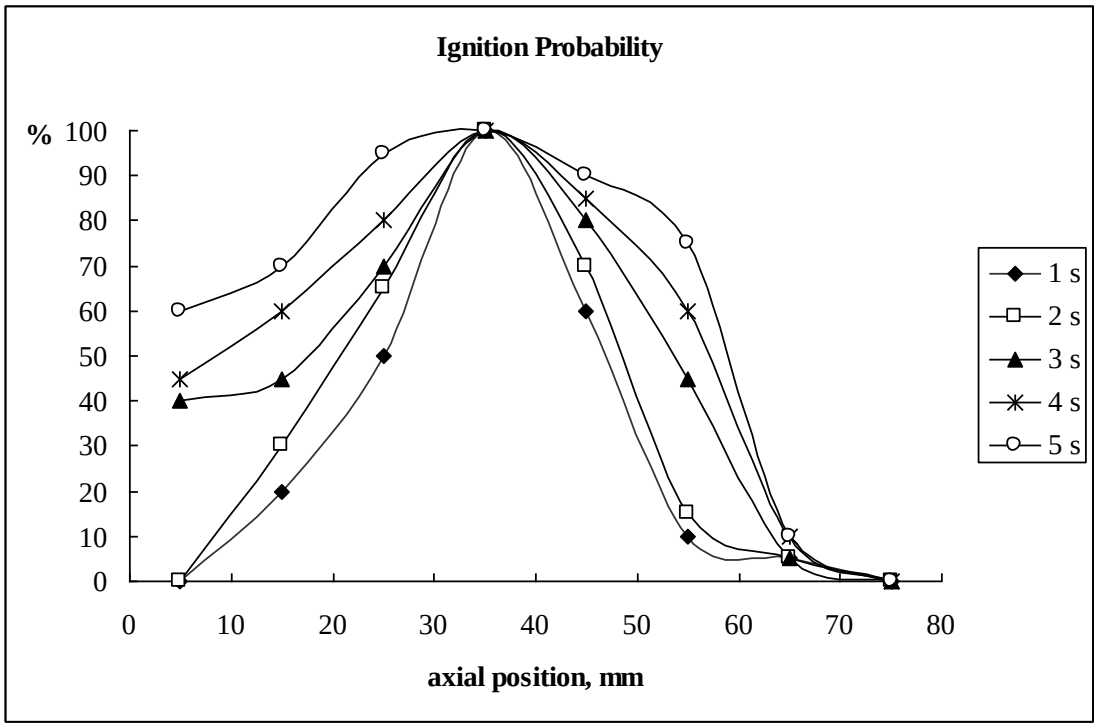

Fig. 6 Ignition probability (%) for a spark sequence of the indicated duration as a function of axial location of the spark. For all, the spark was placed 5mm from the combustion chamber enclosure, i.e. at a radius of 30mm.

For 1 and 2s sequences, the ignition probability is zero at 5mm from the burner. It then starts to increase to the maximum value of 100% at Z_s=35 mm from the burner (i.e. one burner diameter) and then it decreases to zero at Z_s=70mm. When the duration time is higher than 2 seconds, the ignition probability values increase everywhere and even at Z_s=5mm from the burner where there is no ignition with the 1 and 2s sequences. There, the ignition probability rises to 60% with a 5s sequence. It is evident that high spark frequency increases the ignitability of the spray for all spark positions.

The highest value of 100% at Z_s=35mm is achieved independently from the duration of the spark sequence. This location corresponds to a Sauter mean diameter of the droplets around 40-45 μm, high swirl and positive axial velocity. The rapid decrease of the ignition probability at large Z_s is consistent with the increase in Sauter mean diameter (Fig. 4). Note that the maximum ignition probability coincides with the location of maximum width of the recirculation zone (Fig. 2). This is consistent with spark ignition of gaseous recirculating flames [14] and with the conjectures on the effects of swirl offered in the previous section.

The PDA system showed a very different validation data rate at various locations in the burner and a wide PDF of droplet size and velocity. These imply that the droplet-air mixture at the spark can instantaneously be very different than the one that could be inferred from the mean quantities, which in turn implies that the spark's energy may not always be higher than the minimum ignition energy required. This may be an additional reason why some sparks in Fig. 5 do not result in a flame and why the ignition probability is not unity everywhere. However, lack of kernel generation is clearly not the only reason, since Fig. 5 contains events where kernels exist but do not establish a flame. The local equivalence ratio and its fluctuations are necessary to elucidate this further. In order to fully understand the present results and our previous ignition probability data with a single spark in the bulk of the flow [15], it is important to measure the local equivalence ratio of the droplet-air mixture and it would be advantageous to have a separate measurement of the fuel vapour only.

Conclusions

This paper examined the use of multiple sparks in an n-heptane spray in a swirling recirculating flow typical of a liquid-fuel burner. The spark was located close to the combustion chamber enclosure. Spark discharges each lasting 8ms at 100Hz were created in the 5mm gap between two stainless steel 1mm diameter electrodes connected to a coil. The spark sequence lasted from approximately 1 to 5s, hence a total of about 100 to 500 sparks were used. Phase and Laser Doppler Anemometry measurements of the droplet size and velocity and of the air axial and swirl velocity showed a large central recirculation zone, with high swirl velocity at the spark location and a stagnation point of the outer recirculation zone on the enclosure at about 10mm from the burner inlet. It was found that a long spark sequence increases the ignition probability, which reached a maximum of 100% at an axial distance of about one burner inlet diameter. Ignition in the outer recirculation zone was possible only with spark sequences of duration longer than 2s, while all sequences tested produced no ignition downstream of about two burner diameters. Imaging with a fast camera showed that small flame kernels emanate very often from the spark, which can be stretched as far as 20mm from the electrodes by the turbulent motion. Successful ignition is associated with kernels that propagate towards the bluff body to stabilize the whole flame. The results demonstrate that the energy deposited by multiple sparks can have a spatially far-reaching effect to initiate combustion.

Acknowledgements

This work has been funded by the EU project TIMECOP-AE (AST5-CT-2006-030828).

References

[1] Spalding, D.B., *Combustion and mass transfer*, Pergamon Press, Oxford, 1979.
[2] Lefebvre, A.H., *Gas turbine combustion*, 2nd Edition, Taylor and Francis, London, 1998.
[3] Baum, M. and Poinsot, T.J., *Combust. Sci. and Tech.,* **106:**19-39 (1995).
[4] Aggarwal, S.K., *Prog. Energy Combust. Sci.*, **24:**565-600 (1998).
[5] Ballal, D.R. and Lefebvre, A.H., *Proc. Combust. Inst.,* **15**:1473-1481 (1975).
[6] Ballal, D.R. and Lefebvre, A.H., *Proc. Roy. Soc. Lond. A,* **357**:163-181 (1977).
[7] Ballal, D.R. and Lefebvre, A.H., *Combust. Flame,* **35**:155-168 (1979).
[8] Ballal, D.R., and Lefebvre, A.H., *Proc. Combust. Inst.,* **18**:1737-1746 (1981).
[9] Richardson, E.S. and Mastorakos, E., *Combust. Sci. and Tech.,* **179**:21-37 (2007).
[10] Chakraborty, N., Mastorakos, E., Cant, R.S., *Combust. Sci. and Tech.,* **179**:293-317 (2007).
[11] Ahmed, S.F. and Mastorakos, E., *Combust. Flame,* **146**:215-231 (2006).
[12] Ahmed, S.F., Balachandran, R., Mastorakos, E., *Proc. Combust. Inst.,* **31**:1507-1513 (2007).
[13] Birch, A.D., Brown, D.R., Dodson, M.G., *Proc. Combust. Inst.* **18:**1775-1783 (1981).
[14] Ahmed, S.F., Balachandran, R., Marchione, T., Mastorakos, E., Spark ignition of turbulent non-premixed bluff-body flames. Submitted to *Combust. Flame*, 2007.
[15] Marchione, T., Ahmed, S.F., Balachandran, R., Mastorakos, E., *21st ICDERS*, Poitiers, France, July 2007.
[16] Anon, *KLG ignition equipment, igniters and glow plugs,* Technical Report Smiths Aviation Division Maintenence Manual 74-20-102/01, 1961.
[17] Lewis, B. and Elbe, G.V., *Combustion, Flames and Explosions of Gases*, Harcourt Brace Jovanovich, Publishers, London, 1987.